Peptide cross-linked poly(2-oxazoline) as a sensor material for the detection of proteases with a Quartz Crystal Microbalance

Norlaily Ahmad [1,5]*, Burcu Colak* [1]*, Martin John Gibbs* [1]*, De-Wen Zhang* [2]*, Julien E. Gautrot* [1]*, Michael Watkinson* [3]*, C. Remzi Becer* [4]*, Steffi Krause* [1]*

[1] School of Engineering and Materials Science, Queen Mary University of London, London, E1 4NS, UK

[2] Institute of Medical Engineering, School of Basic Medical Sciences, Xi'an Jiaotong University Health Science Center, Xi'an, 710061, China

[3] The Lennard-Jones Laboratories, School of Chemical and Physical Sciences, Keele University, Staffordshire, ST5 5BG, UK

[4] Department of Chemistry, University of Warwick, Coventry, CV47AL, UK

[5] Centre of Foundation Studies, Universiti Teknologi MARA, Cawangan Selangor, Kampus Dengkil, 43800 Dengkil, Selangor, Malaysia

* Corresponding author: s.krause@qmul.ac.uk, Telephone +44 (0)20 78823747

ABSTRACT

1

Inflammatory conditions are frequently accompanied by increased levels of active proteases, and there is rising interest in methods for their detection to monitor inflammation in a point of care setting. In this work, new sensor materials for disposable single-step protease biosensors based on poly(2-oxazoline) hydrogels cross-linked with a protease-specific cleavable peptide are described. The performance of the sensor material was assessed targeting the detection of matrix metalloproteinase-9 (MMP-9), a protease that has been shown to be an indicator of inflammation in multiple sclerosis and other inflammatory conditions. Films of the hydrogel were formed on gold coated quartz crystals using thiol-ene click chemistry, and the cross-link density was optimised. The degradation rate of the hydrogel was monitored using a quartz crystal microbalance (QCM) and showed a strong dependence on the MMP-9 concentration. A concentration range of 0-160 nM of MMP-9 was investigated and a lower limit of detection of 10 nM MMP-9 was determined.

Introduction

Monitoring the degradation of hydrogel films is a promising platform for disposable biosensors capable of measuring protease activity. Elevated levels of proteases have been linked to a variety of inflammatory conditions including multiple sclerosis (MS), periodontal disease, bacterial infection in catheters, anaphylaxis and solid organ graft rejection [1–7]. Hence, there is significant interest in the development of effective sensor technologies for the detection of these enzymes. Single-step sensors that can be used in a point of care setting at a doctor's surgery or for home monitoring of inflammation are particularly sought after.

Poly(2-oxazolines), are a class of poly(ethylene glycol) (PEG) analogues that has been reported to reduce the immunogenic properties of BSA [8] and displays excellent anti-fouling

2

properties [9,10]. They have been proposed for cell growth support [11], cell delivery [12], drug delivery applications [13,14] and the immune capture [15]. Given their anti-fouling properties, poly(2-oxazolines) are attractive materials for the development of biosensors as interference of proteins during sensing and the associated lack in specificity and sensitivity are expected to be reduced. Hence, this work focuses on the development of peptide cross-linked poly(2-oxazoline) as a new class of sensor material for the detection of proteases. 'Click chemistry' has been intensively reviewed as a tool for facile functionalization of materials [16,17]. The use of thiol-ene click chemistry as a cross-linking method to prepare the biosensor material is promising as it has been reported to react effectively at low concentrations and under mild conditions [18–20].

The target protease chosen for this work is matrix metalloproteinase-9 (MMP-9), which is a biomarker for heart disease, cancer, autoimmune diseases and mostly linked to inflammation [21–25]. For example, in MS, which is a chronic inflammatory demyelinating autoimmune disorder of the central nervous system (CNS) [26], several studies showed that active MMP-9 serum levels were higher in patients of relapsing-remitting MS (830 µM) compared to healthy controls (540 µM) [27–29].

Film degradation by an enzyme has been monitored previously in a disposable sensor format using a quartz crystal microbalance (QCM), impedance spectroscopy and surface plasmon resonance [30–33]. Natural substrates, i.e. proteins, have been used as protease activity sensors based on film degradation [31,34–38]. However, proteins only allow for limited specificity as they contain multiple cleavage sites that can be degraded by proteases other than the target protease.

The use of hydrogels cross-linked with peptides that contain cleavage sites for specific proteases has been described previously [30,32,33,39]. While polyacrylamide hydrogel cross-linked with the peptide AAPVAAK showed relatively low sensitivity to human neutrophil

elastase (HNE), greater sensor responses were observed with peptide cross-linked oxidised dextran hydrogel films, the degradation of which was monitored using QCM and impedance measurements at interdigitated electrodes (IDEs) [30,32,39]. Oxidized dextran cross-linked with different peptides showed sensitivity to biomarkers of periodontal disease such as HNE, cathepsin G and MMP-8 [30,32]. MMP-9 has been detected using impedance measurements at IDEs coated with LGRMGLPGK cross-linked oxidised dextran hydrogel films in a concentration range of 0.54 to 4.3 nM MMP-9 [39]. Drawbacks of this material were a delayed QCM response at low enzyme concentrations when the film was produced in a single coating step [30] or a lack of stability of the QCM signal before enzyme addition when the film was produced in separate deposition steps of oxidized dextran and peptide [32]. Dextran is a natural polymer and contains aldehyde groups in its oxidized form, which may also cause unwanted binding of proteins and its properties cannot be tailored as easily as that of synthetic polymers. Therefore, new synthetic polymers cross-linked with enzyme-selective peptide sequences are promising as biosensor materials as they offer great flexibility compared to natural substrates and can be readily optimized to maximize the sensor response. A collagenase biosensor based on a peptide cross-linked four-armed PEG has recently been described, although the effects of non-specific binding were not investigated for this system [40].

In this study, a peptide cross-linked poly(2-oxazoline) hydrogel was developed as a biosensor material for the detection of proteases using MMP-9 as a model analyte. Film degradation in the presence of MMP-9 was monitored with QCM measurements.

2. Materials and methods

2.1 Materials

The following chemicals were purchased from Sigma-Aldrich, UK: Tricine (*N*-[tris(hydroxymethyl)methyl]glycine, 99%), sodium chloride (99.5%), calcium chloride

dihydrate (99%), MES hydrate (4-morpholineethanesulfonic acid, 99.5%), pentenoic acid (97%), anhydrous toluene (99.8%), 3-(trimethoxysilyl)propyl methacrylate (98%), trichloro(octadecyl)silane (90%), bovine serum albumin (BSA, lyophilized powder, 96%), triethylamine (99%), 4-pentenoyl chloride (98%), 2-chloroethylamine hydrochloride (99%), 2-ethyl-2-oxzoline (99%), methyl *p*-toluenesulfonate (97%), deuterium oxide (99.9% atom% D), anhydrous magnesium sulfate (99.5%), sodium bicarbonate (99.7%), hydrochloric acid (37%), dichloromethane (99.5%), anhydrous acetonitrile (99.8%), anhydrous dichloromethane (99.8%), anhydrous methanol (99.8%), diethyl ether (99%), and Irgacure 2959 (2-hydroxy-4'-(2-hydroxyethoxy)-2-methylpropiophene, 98%). Chloroform-D (99.8%) was purchased from Cambridge Isotope Laboratories Inc. Zinc chloride, concentrated sulfuric acid (95-98%) and hydrogen peroxide (30% H_2O_2 (w/w)) were purchased from Fluka. Sodium hydroxide (1 M) was purchased from Fisher Chemicals, UK. The peptide used as the cross-linker, Ac-CSG(ac-K)IPRRLTAC (95-98%) with molecular weight 1388.88 Da was synthesized by Genscript Ltd. (Hong Kong). MMP-9 catalytic domain (39 kDa, purity ≥95%), MMP-2 catalytic domain (40 kDa, purity ≥90), fluorogenic substrate, Mca-KPLGL-Dpa-AR-NH_2 (98%), and OmniMMP[TM] fluorogenic control, Mca-PL-OH (98%), were purchased from Enzo Life Sciences (UK) Ltd. Microscopic glass slides (Menzel-glaser, 75 mm x 25 mm) used in sensor fabrication were purchased from Thermo Scientific. Round glasses cover slips (20 mm) were purchased from VWR. Polished, gold coated QCM crystals (AT-cut, 10 MHz) were purchased from the International Crystal Manufacturing Company, Inc (USA). Milli-Q water (resistivity 18.2 MΩ.cm) was used to prepare all the solutions and to rinse the glassware.

2.2 Standard analysis techniques

^{1}H-NMR spectra were measured using Bruker AV400 and AVIII400 spectrometers with abbreviations for the peaks: t-triplet and m-multiplet. ATR-FTR measurements were

conducted using a Bruker Tensor 27 spectrometer equipped with an MCT detector and spectra were obtained between 600 and 4000 cm^{-1}. GPC analysis was obtained using an Agilent 1260 infinity system operated in DMF with NH_4BF_4 (5 mM) and equipped with refractive index and variable wavelength detectors, 2 Plgel 5 μm mixed-C column (300 x 7.5 mm), a Plgel 5 mm guard column (50 x 7.5 mm). The instrument was calibrated with poly(methyl methacrylate) standards between 5.5 and 46.9 kg/mol. All samples were passed through 0.2 μm nylon 66 filters before analysis.

2.3 MMP-9 and MMP-2 activity

The enzymatic activity of MMP-9 and MMP-2 at 25°C in tricine buffer (100 mM, pH 7.4) containing 100 mM NaCl, 10 mM $CaCl_2$, 50 μM $ZnCl_2$ was measured based on the degradation of a fluorogenic substrate using a FLUOstar microplate reader over 8 min. The fluorogenic control substrate was used to construct the calibration curve and the degradation rate (pmoles/min) was measured. The calibration curve (Relative fluorescene units, RFU versus concentration of enzymes, pmoles) gave a linear regression with equation $y = 259 x + 106$ ($r^2 = 0.999$). The enzyme assay using 20 nM (780 μg/ml) of MMP-9 gave a degradation rate of 2.57 pmol/min and 1.60 pmol/min for 20 nM (800 ng/mL) of MMP-2.

2.4 Peptide degradation

Prior to the preparation of hydrogel films, the peptide sequence, Ac-CSG(ac-K)IPRRLTAC, was first shown to be degraded by MMP-9. Throughout this investigation, the acetyl protecting groups remained intact. However, thiol from cysteine was reported to inhibit MMP-9 activity by chelating a zinc-containing active site [41,42]. Thus a capping method was introduced (Scheme S1); 4-pentenoic acid (PA) was used to cap both cysteines at the terminals of the peptide sequence. PA (90 μmol, 90 mM) was reacted with peptide (45 μmol in MES buffer, 45 mM) using the UV thiol-ene click reaction. 5 mol % of photo-initiator, Irgacure 2959 (2.5 mM, 12.5 μL from 250 mg/mL) was added into the solution and UV-

cured for 300 s. 100 µM of the product formed (modified peptide, X) was incubated with 25 nM MMP-9 in tricine buffer solution for 3 hours at 37°C. The sample before and after degradation was measured using a matrix assisted laser desorption/ionisation-time of flight mass spectrometer (MALDI-ToF MS).

2.5 Synthesis of poly(2-oxazoline) co-polymer (pOx)

2-(3-Butenyl)-2-oxazoline monomer (M1) was synthesised as described by Gress et al.[43] (Scheme S2). Briefly, 2-chloroethylamine hydrochloride (R1, 10.6 g, 1.2 eq., 93.1 mmol) was dissolved in anhydrous dimethylformamide (80 mL) and the solution was cooled to 0 °C. Triethylamine (R2, 19.6 g, 2.5 eq., 194 mmol) was added, followed by dichloromethane (75 mL) and pentenoyl chloride (9.12 g, 1 eq., 77.6 mmol). The reaction was stirred in an ice/water bath for 24 h under an inert nitrogen atmosphere and allowed to warm up to room temperature. To this mixture, dichloromethane (200 mL) was added and the combined organic phases were washed with hydrochloric acid (1M, 500 mL four times), saturated sodium bicarbonate solution (500 mL twice) and brine (500 mL four times) then dried over magnesium sulfate to yield *N*-(2-chloroethyl)-4-pentenamide (R3) as a brown oil. Crushed potassium hydroxide (4.48 g, 1 eq., 79.8 mmol) was added into an oven dried flask and purged with nitrogen. Dry methanol (40 mL) was added and then R3 (12.9 g, 1 eq., 79.8 mmol) was introduced. The mixture was then heated at 70 ºC for 24 h. The salts were separated by filtration and the organic phase concentrated *in vacuo*. The crude product was purified by distillation (82 °C, 6 mbar) from calcium hydride to yield M1 as a clear oil.

The poly(2-oxazoline) co-polymer (pOx) was synthesised as reported previously [44]. Briefly, 2-ethyl-2-oxazoline (M2) was distilled from calcium hydride (7.93 g, 80 eq., 80.0 mmol), M1 (2.50 g, 20 eq., 20.0 mmol) and anhydrous acetonitrile (20 mL) were measured into a microwaveable flask, to which methyl *p*-toluenesulfonate (R4, 0.186 g, 1 eq., 1.00 mmol) was added. The reaction was heated using a microwave, at 140 ºC for 30 min. The

reaction was terminated by the addition of a drop of water and the product precipitated by the addition of cold (0-4 °C) diethyl ether (500 mL). The remaining polymer was collected by filtration under suction and dried *in vacuo*. Characterisation: *N*-(2-chloroethyl)-4-pentenamide (R3): δ_H (400 MHz; CDCl$_3$) 2.27-2.35 (4H, m, C$\underline{H}_2$-C$\underline{H}_2$-C=O), 3.55 (4H, m, NH-C$\underline{H}_2$C$\underline{H}_2$-Cl), 4.94-5.09 (2H, m, C$\underline{H}_2$=CH) and 5.72-5.90 (1H, m, CH$_2$=C$\underline{H}$); 2-(3-butenyl)-2-oxazoline monomer (M1): δ_H (400 MHz; CDCl$_3$) 2.45 (4H, m, C$\underline{H}_2$-C$\underline{H}_2$-C=N), 3.88 (2H, t, C$\underline{H}_2$-C-O), 4.35 (2H, t, C$\underline{H}_2$-N=C), 4.99-5.12 (2H, m, C$\underline{H}_2$=CH) and 5.90-5.93 (1H, m, CH$_2$=C$\underline{H}$). v/cm^{-1} ~2900 (w, C-H), 1675 (s, C=O), 1174 (w, C-N); poly(2-oxazoline) co-polymer (pOx): δ_H (400 MHz; CDCl$_3$) 1.06-1.22 (3H, m, C$\underline{H}_3$-CH$_2$), 2.21-2.55 (9H, m, C$\underline{H}_3$-N, CH$_3$-C$\underline{H}_2$-C=O, CH$_2$-C$\underline{H}_2$-C=O, and C$\underline{H}_2$-CH$_2$-C=O), 3.28-3.74 (8H, m, N-C$\underline{H}_2$-C$\underline{H}_2$-N), 4.95-5.11 (2H, m, C$\underline{H}_2$-CH) and 5.74-5.89 (1H, m, C$\underline{H}$-CH$_2$). v/cm^{-1} ~3400 (br, O-H), ~2900 (w, C-H), 1633 (s, C=O), 1180 (w, C-N). Co-polymer ratio (M2:M1) was calculated 85:15. Mn 6.3 kg/mol, PDI 1.62.

2.6 Sensor fabrication

2.6.1 Cleaning of QCM crystals

The gold coated QCM crystals were cleaned with piranha solution (a mixture of 3:1, v/v, concentrated sulfuric acid and 30 wt % hydrogen peroxide) for 3 min and then rinsed thoroughly with Milli-Q water three times. The crystals were then blow-dried using nitrogen prior to use.

2.6.2 Functionalised glass slide

A microscopic glass slide was first cleaned using piranha solution for 10 min. The glass slide was rinsed thoroughly using Milli-Q water and dried in an oven at 100 °C for 10 min. The clean glass slide was immersed in a beaker of 0.02% v/v of trichloro(octadecyl)silane in anhydrous toluene for 90 min and closed tightly with Parafilm to avoid moisture absorption.

The modified glass slide was then rinsed with toluene, acetone and lastly with Milli-Q water before blowing dry using nitrogen.

2.6.3 Mixture of peptide and pOx for hydrogels

A stock solution of pOx (303 mg/mL) was prepared in MES buffer (0.2 M, pH 5.5). For 25 % cross-linking with 135 μmol/mL pOx (91.1 mg/mL), a total volume of 200 μL solution was prepared with 60 μL of pOx stock solution mixed with 4.7 mg of peptide cross-linker (33.75 mM, 23.43 mg/mL dissolved in MES buffer, 0.2 M, pH 5.5) to which photo-initiator (Irgacure 2959, 1.69 mM, 0.38 mg/mL, 5 mol %) was added (Table S3). The cross-linking procedure used here was adapted from a thiol-ene click reaction between mono-cysteine peptide sequence and pentenoic acid [18]. To obtain different degrees of cross-linking, 9.4 mg (67.50 mM, 46.87 mg/mL) and 14.06 mg (101.3 mM, 70.31 mg/mL) of peptide were used to achieve 50% and 75% cross-links respectively, keeping the concentration of pOx constant, and 5 mol % (with respect to thiol) of photo-initiator. Hydrogel films were prepared with different pOx concentrations using 180 μmol/mL (121.5 mg/mL) and 225 μmol/mL (151.8 mg/mL) pOx stock solutions. 25% peptide cross-linker and 5 mol % of photo-initiator were mixed into the pOx solution. All the mixtures were kept in the dark after the photo-initiator was added.
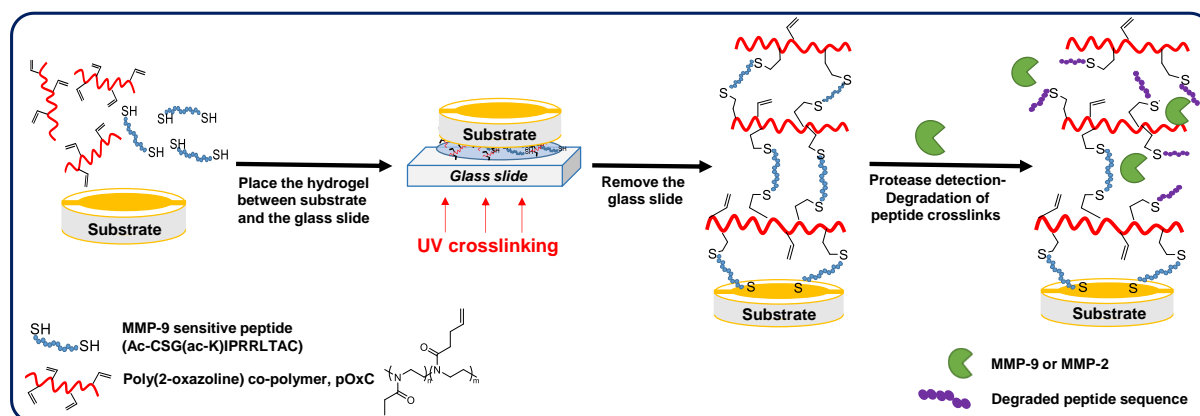
Scheme 1 Sensor fabrication and detection of MMP-9.

2.6.4 Hydrogel deposition

The clean gold coated QCM crystal was coated with hydrogel through UV thiol-ene cross-linking as shown in Scheme 1. 25% cross-linked pOx was deposited by sandwiching 3 µL of solution containing peptide and photo initiator between the clean gold coated QCM surface and the silane-modified glass slide prior to UV-curing for 300 s (17 mW/cm^2, 350-500 nm) using a UV-lamp Omnicure series 1500. The glass slide was used to prevent evaporation and shrinkage of the hydrogel during the curing. The hydrogel film coated QCM crystals were removed from the silane-modified glass slide immediately after UV-curing and were kept in tricine buffer prior to the degradation experiment.

2.7 Hydrogel film characterisation

The mechanical properties of the resulting peptide cross-linked pOx were characterised using photo-rheology (TA Discovery HR-3 hybrid rheometer) with a UV activated setup. Cover slips were cleaned using plasma (10 min) [45]. Then the cover slips were immersed in a solution of 3-(trimethoxysily)propyl methacrylate (0.25 mmol, 60 µL) in anhydrous toluene (20 mL) overnight. The cover slips were then rinsed with toluene, acetone and lastly with Milli-Q water before blow drying using nitrogen. Functionalised cover slips were used to prevent slippage between the hydrogel formed and the measuring surfaces during the rheology measurement [45]. The functionalised cover slip was glued to the top geometry and bottom quartz plate of the rheometer. Then, the hydrogel solution with photo-initiator was sandwiched between the rheometer upper plate and the cover slip within a fixed gap of 250 µm. Oscillation at 1% strain was set for controlled strain mode. UV-irradiation was started after 30 s and kept on for 300 s. The storage modulus of hydrogels with different pOx concentrations and different degrees of cross-linking were measured during this time.

X-ray photoelectron spectroscopy (XPS) was performed on a gold coated QCM crystal coated with 25% cross-linked pOx (135 µmol/mL) at Thermo Fisher Scientific, UK, and the

spectrum was analysed using the Advantage software. Survey scans were carried out over a 1100 ~ 0 eV range and the region of sulfur binding energy was analysed in detail to confirm the formation of thioether bonds after the cross-linking. The thickness of the hydrogel on the QCM crystals was measured using a Dektak Surface Profiler (Bruker) and analysed using Vision64 software from Bruker.

2.8 Experimental setup for QCM measurements

QCM measurements were conducted using the experimental setup described by Sabot and Krause[46]. One full quartz crystal admittance spectrum (402 points, acquisition time 1s, ac stimulus 160 mV) was recorded over a range of 20 kHz centered at the QCM resonance frequency (~10 MHz) every 10 s. To monitor hydrogel degradation by MMP-9, the measurement was performed in a customised cell at room temperature (25 °C). 140 µL of tricine buffer was added into the cell and QCM data were recorded 10 min prior to enzyme exposure. 10 µL of enzyme solution was added into the cell and the degradation was monitored for an hour. For the setup, 420 scan points were recorded for the entire experiment over 80 min. A control was run for the degradation by replacing enzyme solution with 10 µL of tricine buffer, recorded as 0 nM MMP-9. The QCM admittance spectra were recorded before and after degradation. The QCM admittance spectra where then fitted with a Butterworth Van Dyke (BVD) equivalent circuit as described by Sabot and Krause [46]. Two QCM parameters were used to describe the degradation of the hydrogel, which is the change in resistance, ΔR, and the change in reflective inductance, $\omega\Delta L$. The change in resistance, ΔR, represents the viscoelasticity of the hydrogel or energy loss due to damping and the change in reflective inductance, $\omega\Delta L$, represents the mass loss of the hydrogel during the degradation.

A set of sensors fabricated using the functionalised glass slide method were prepared for the calibration of the sensor using a range of 0 nM to 160 nM of MMP-9. The selectivity of the sensor and the effects of percentage cross-links, pOx concentration, and the presence of

bovine serum albumin (BSA) on the MMP-9 response were also investigated using sensors fabricated by the functionalised glass slide method. The degradation was monitored before and after the addition of MMP-9 over 60 min.

2.9 Statistical analysis

Results were analysed using T-test and analysis of variance (ANOVA)/post-hoc analysis by Tukey HSD test. Statistical data analysis was carried out using SPSS software version 22.0 and a statistically significant difference was denoted by $p<0.05$. Data were processed based on the average changes of ΔR and $\omega \Delta L$ within 60 min of MMP-9 addition.

3. Results and discussion

To obtain films that degraded in the presence of MMP-9, a suitable peptide cross-linker for pOx had to be selected. For this work, the SGKIPRRLTA peptide sequence was chosen as the cross-linker due to its good sensitivity to MMP-9 and MMP-2 with the cleavage site situated between arginine and leucine. The catalytic efficiencies of this peptide sequence to MMP-9 and MMP-2 have been reported with k_{cat}/K_m 1.6×10^5 M^{-1} s^{-1} [47] and k_{cat}/K_m 3.8×10^4 M^{-1} s^{-1} [48], respectively. In order to enable this peptide sequence to be incorporated into polymeric cross-linked biosensor substrates, cysteine residues were added at both *N*- and *C*-peptide terminals. The cysteine (*N*-terminal) and the lysine residue within the peptide sequence were acetylated to protect free amines from reacting during the cross-linking reactions. The degradation of the peptide (X, (ac-C)SG(ac-K)IPRRLTAC) by MMP-9 was confirmed by MALDI-ToF MS analysis, with the presence of a new molecular ion (Y, (ac-C)SG(ac-K)IPRR) observed at *m/z* 1102.1, which corresponds to the degraded peptide sequence (Fig. S4).

3.1 Characterisation of hydrogel films

The lowest degree of cross-linking required for gelation was determined to be 25% as confirmed by carrying out the UV thiol-ene click coupling in a vial (Fig. S5). The result

shows that the hydrogel was formed in 300 s under UV-irradiation. Photo-rheology confirmed the rapid evolution of the pOx hydrogel as a function of time after exposure to UV (Fig. 1a and 1b). As shown in Fig. 1a, the storage modulus increased sharply after UV-light was turned on after 30 s for 50% and 75% cross-linking. However, the storage modulus for 25% cross-linking increased slowly with a lower final value of the storage modulus. The same trend was observed with the pOx concentration (Fig. 1b) which shows that the storage modulus increased slowly at 135 μmol/mL compared to 180 and 225 μmol/mL. 25%, 50%, and 75% cross-linked pOx hydrogels prepared with 135 μmol/mL pOx resulted in storage moduli of 81.61 ± 3.258 Pa, 4964 ± 428.0 Pa, and 7533 ± 335.8 Pa, respectively. 135 μmol/mL, 180 μmol/mL and 225 μmol/mL of pOx concentration resulted in storage moduli of 81.61 ± 3.258 Pa, 299.0 ± 19.83 Pa and 1400 ± 629.4 Pa. An increase of initial reactant concentration in the hydrogel mixture resulted in an increase of the cross-linking efficiency and, therefore, an increase of the storage modulus [49].

Fig. 1c displays the narrow scan XPS spectrum for sulfur 2p of the 25% cross-linked pOx hydrogel film coated on a QCM crystal. The XPS spectrum was fitted with 2 components, where each component has a doublet S $2p_{3/2}$ and S $2p_{1/2}$ with an energy separation of 1.2 eV and an intensity ratio of 2:1. The fitted S $2p_{3/2}$ peaks were assigned to Au-S (~162.40 eV) and S-C (~163.59 eV) which is in agreement with previous studies [50–52]. The S-C peak reported here belongs to C-S-C, which was reported previously in the region of 163.4-163.6 eV [53]. In conclusion, the S-C peak confirmed the formation of carbon-sulfur bonds between the alkene from pOx and the thiol from the cysteine residue in the peptide cross-linker. The unreacted peptide was dissolved in water and washed away during the rinsing process. The average thickness of these hydrogel films was 0.594 μm ± 0.042 μm.
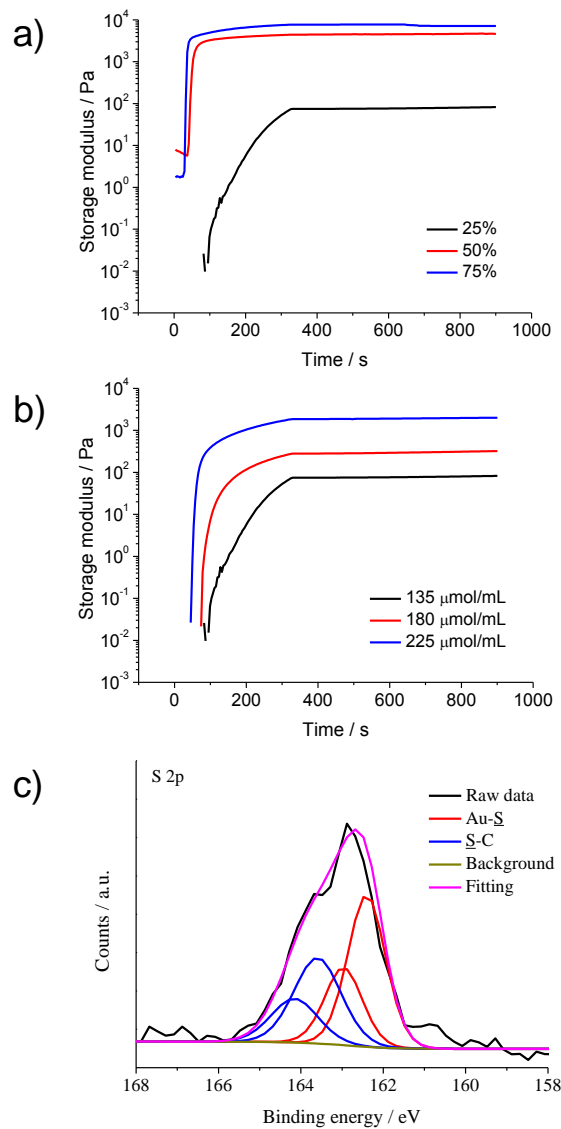
Fig. 1 (a) The evolution of the storage modulus as a function of time for different percent cross-linking with 135 μmol/mL and (b) 25% cross-linked with different pOx concentration. (c) XPS spectrum of gold coated QCM crystal coated with 25% cross-linked pOx.

3.2 Optimisation of the peptide cross-linked pOx hydrogel

3.2.1 The effect of the degree of cross-linking on the MMP-9 sensor response

Hydrogel films with various percentages of peptide cross-links in a range from 25% to 75% were obtained by changing the concentration of peptide in the pOx solution, and their

degradation before and after addition of 20 nM MMP-9 was monitored using QCM measurements, which were performed in a custom cell at room temperature (Fig. 2a-c). The degree of cross-linking referred to is defined by the stoichiometric feed ratio of thiol groups in the peptide to alkene groups in the pOx. The hydrogel was first equilibrated in tricine buffer for 1 h before exposure to MMP-9 to allow the film to stabilise before the enzyme was added. A small increase of both the resistance ΔR and the reactive inductance $\omega\Delta L$ was observed immediately after the addition of the enzyme, which corresponded to the enzyme binding to the hydrogel. The degradation of hydrogels was strongly dependent on the percentage of peptide cross-links. An increase of the percentage cross-linking caused a decrease in the sensor response. At 25%, 50% and 75% cross-linking, the ΔR at 60 min observed were -8.0 Ω, -5.2 Ω and +0.6 Ω, respectively. The average sensor response, ΔR, shows a significant difference between different percentages of crosslinking (ANOVA, p<0.05). This trend was observed as the hydrogels with lower percentage cross-linking had more porous hydrogel structures compared to the higher percentage cross-linking, thus allowing better access of the MMP-9 to the peptide cross-links and resulting in faster degradation. A similar trend was reported by Schyrr et al. [38], where a higher sensitivity of an MMP-2 optical sensor was observed at a lower cross-linking concentration of glutaraldehyde in gelatine. For a recently reported collagenase sensor based on peptide cross-linked four-armed PEG, the opposite trend was observed yielding the highest sensitivity at the highest cross-link density [40]. It is assumed that this difference was caused by larger pore sizes due to the four-armed architecture of the PEG and possibly the greater hydrophilicity of the peptide allowing the enzyme to enter the hydrogel even at high cross-link densities. The linear architecture of the pOx used in this work most likely resulted in smaller pore sizes at high cross-link densities. At the highest cross-link density of 75%, a small increase in both resistance ΔR and the reactive inductance $\omega\Delta L$ was observed. This is most likely due to

swelling caused by the cleavage of cross-links without significant dissolution of the film and subsequent influx of water into the surface regions of the hydrogel.

A comparison of the changes in the reactive inductance $\omega\Delta L$ and the resistance ΔR (Fig. 2a and b) shows that the changes in $\omega\Delta L$ were about three times smaller than the changes in ΔR. This could be caused by the poor mass coupling of the hydrogel to the quartz crystal due to the high viscoelasticity of the hydrogel. The decrease in $\omega\Delta L$ corresponds to mass loss as the hydrogel started to be degraded by the enzyme through the cleaving of the peptide cross-linker. The fragments of the degraded hydrogel then dissolved into the tricine buffer. A decrease in ΔR indicates that the energy loss due the damping caused by the hydrogel film decreased as the film degraded. Interestingly, in contrast to the results obtained here, a peptide cross-linked four-armed PEG described recently [40] only showed a change in ΔR but no significant mass loss upon degradation with collagenase. It was assumed that this was due to the binding of the enzyme to the partially degraded hydrogel, which also resulted in incomplete degradation. This does not appear to be the case for the MMP-9 response of the peptide cross-linked pOx in this work where the degradation continues over the entire measurement period.

3.2.2 The effect of the pOx concentration during cross-linking on the MMP-9 sensor response

The effect of the pOx concentration during hydrogel formation with 25% of peptide cross-links on the degradation rate upon exposure to MMP-9 is shown in Fig. 2d-f. Degradation was measured for 60 min using 20 nM MMP-9 for each hydrogel. Films were prepared with 135, 180 and 225 μmol/mL of pOx concentration cross-linked with 25% peptide. From Fig. 2d and e, the increase of pOx concentration resulted in a decrease of $\omega\Delta L$ and ΔR. Fig. 2f shows a significant difference in average sensor response, ΔR, between different pOx concentrations (ANOVA, $p<0.05$). Again, the changes in $\omega\Delta L$ were about three times smaller

16

than the changes in ΔR. The hydrogel synthesised with 225 μmol/mL of pOx showed the lowest response with about 0 Ω in good agreement with the response observed at different cross-link densities. It is proposed that both, increasing the concentration of pOx and increasing the cross-link density, decreases the porosity of the hydrogel film, thereby reducing the accessibility of cross-links to the enzyme. As the ΔR change was more significant than that of $\omega\Delta L$, the following results will be discussed using the ΔR values.
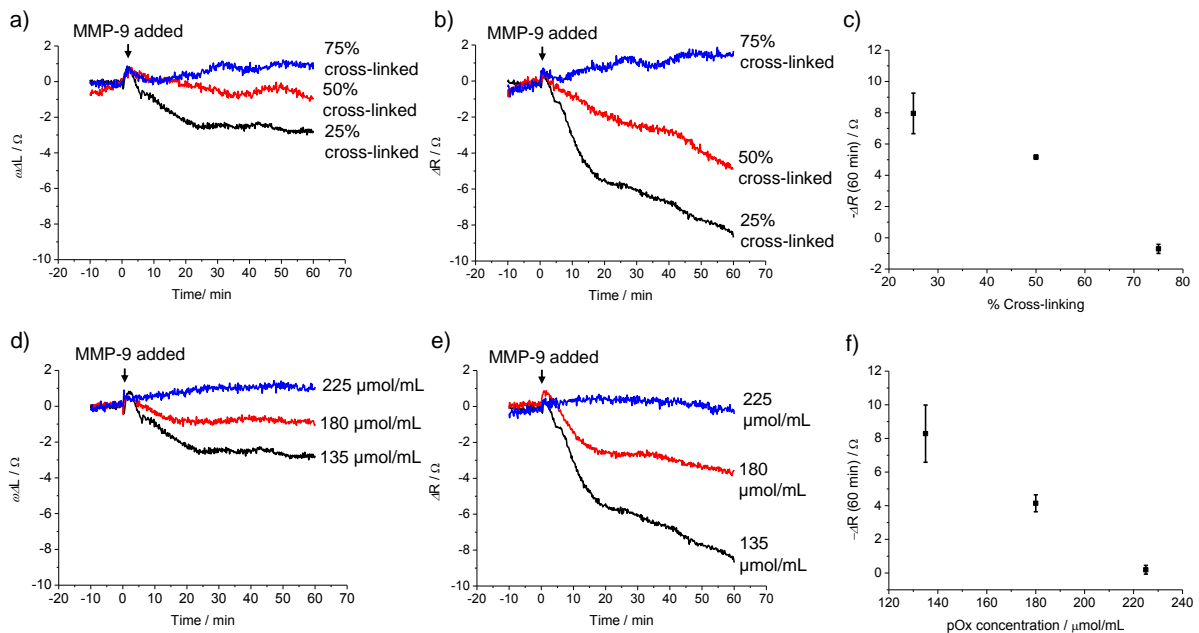

Fig. 2 QCM response, (a) $\omega\Delta L$ and (b) ΔR of 25%, 50%, and 75% CSGKIPRRLTAC cross-linked pOx (135 μmol/mL) before and after addition of 20 nM MMP-9 at $t = 0$. (c) Average of ΔR for different degrees of cross-linking after 60 min incubation. QCM response, (d) $\omega\Delta L$ and (e) ΔR of 25% cross-linked films with different concentrations of pOx: 225, 180 and 135 μmol/mL after addition of 20 nM MMP-9 at $t = 0$. (f) Average of ΔR for hydrogel films made with different pOx concentrations in 60 min. The error bars represent the standard deviation for n=3.

17

3.3 Concentration dependent MMP-9 response of the hydrogel

The optimised hydrogel was exposed to different concentrations of MMP-9 (Fig. 3a). Comparatively, no degradation response of the hydrogel was observed over the same time period in tricine buffer without MMP-9, which demonstrated the hydrogel stability over the degradation time. With increasing MMP-9 concentration, the rate and the extent of the decrease in $\varDelta R$ increased. The degradation was observed to be faster at the beginning and then became slower. The continued change in $\varDelta R$ indicates that the degradation was incomplete within the 60 min measurement window. For the hydrogel that was exposed to 160 nM MMP-9, the higher rate of degradation lasted for 30 min and for 10 nM MMP-9, it lasted for 13 min. This may be caused by the zinc atom at the active site of the enzyme coordinating to the unreacted cysteine of the peptide resulting in deactivation of the enzyme. Based on these results, it can be seen clearly that MMP-9 concentrations as low as 10 nM can be detected using this system. The lower limit of detection is defined as the concentration at which a response significantly different from the blank response was obtained. The sensor response, $\varDelta R$, shows a significant difference between 0 nM (blank response) and 10 nM (T-test, $p < 0.05$). A calibration curve was plotted using the change in resistance, $\varDelta R$, at 60 min of hydrogel degradation at various MMP-9 concentrations (Fig. 3b) showing a linear relationship. To investigate the effect of non-specific binding, multiple concentrations of BSA were added to the sensor. No significant change of ΔR or $\omega\Delta L$ was observed indicating that BSA does not bind to the film (Fig. 3c).
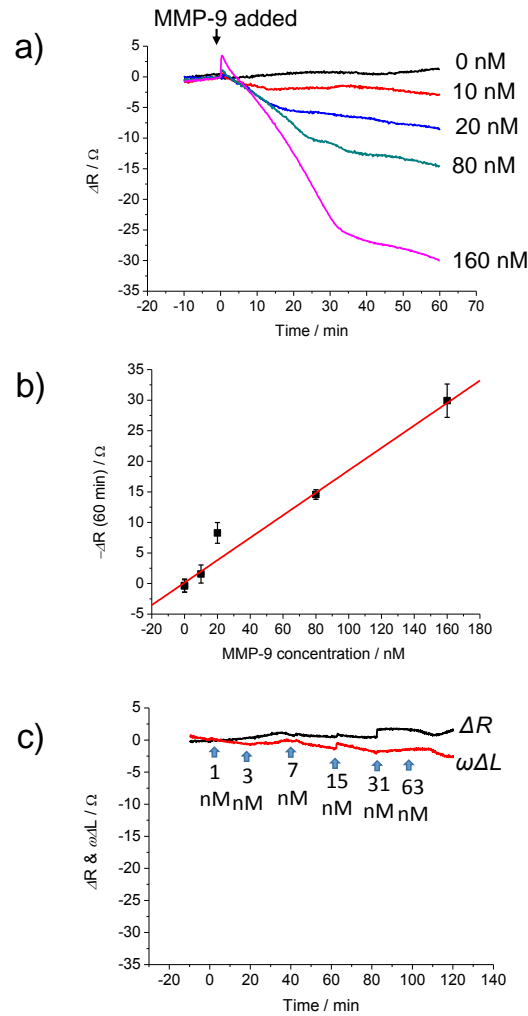
Fig. 3 (a) QCM response, ΔR for 25% peptide cross-linked pOx after exposure to different concentrations of MMP-9 in a range of 0-160 nM. (b) The linear regression between the average ΔR value at 60 min and the MMP-9 concentration based on the QCM response in panel (a) (y = 0.183 x + 0.147 (r^2 = 0.965)). The error bars represent the standard deviation for n=3. (c) QCM response, ΔR and $\omega\Delta L$ for 25% peptide cross-linked pOx after exposure to different concentrations of BSA.

3.4 Cross-sensitivity studies using MMP-2 and MMP-9

Chen *et al.*[48] reported that the peptide sequence SGKIPRRLTA was sensitive towards both MMP-9 and MMP-2. Here, the optimised sensor was tested with MMP-2, known as gelatinase A, which was reported to be detected in MS but in a different subtype with MMP-9

[27]. No sensor response was observed after exposure to 20 nM MMP-2 over 60 min as in Fig. 4. At 160 nM, MMP-2 shows about 30% reduction of the sensor response compared to MMP-9, which is in line with the activities that were measured with both enzymes. Where clinical applications demand complete differentiation of MMP-2 and MMP-9, selectivity could be achieved by using sensor arrays with different peptide cross-linkers, by further modifying the polymer scaffolds or through a combination of both.
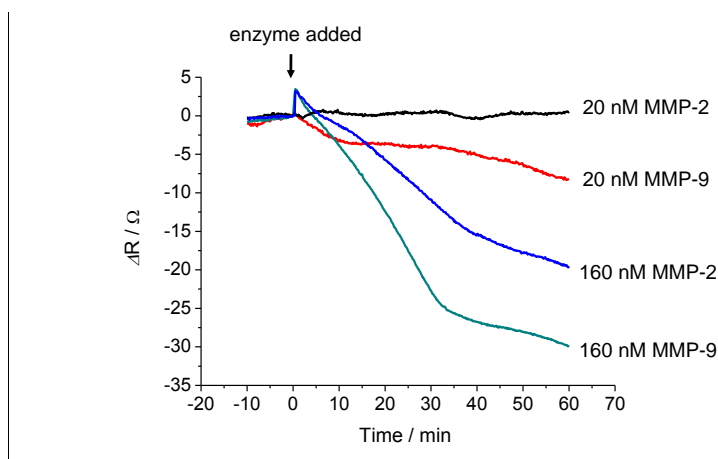

Fig. 4 QCM response, ΔR of 25% cross-linked pOx (135 µmol/mL) with 20 nM and 160 nM of MMP-9 and MMP-2.

3.5 Effect of BSA on the MMP-9 sensor response

Fig. 5 shows the effect of 1% BSA on the degradation of the optimised hydrogel of 25% peptide cross-linked pOx with 20 nM and 160 nM MMP-9. The sensor response, ΔR, after addition of MMP-9 in tricine buffer was -8.7 Ω and -30.0 Ω for 20 nM and 160 nM MMP-9, respectively. In the presence of 1% BSA, the sensor response was still significant, but decreased to -3.1 Ω and -18.6 Ω for 20 nM and 160 nM MMP-9, respectively. It is assumed that this reduction in the sensitivity was caused by the increase of viscosity of solution due to the high protein concentration as BSA does not bind to the film (see Fig. 3c).
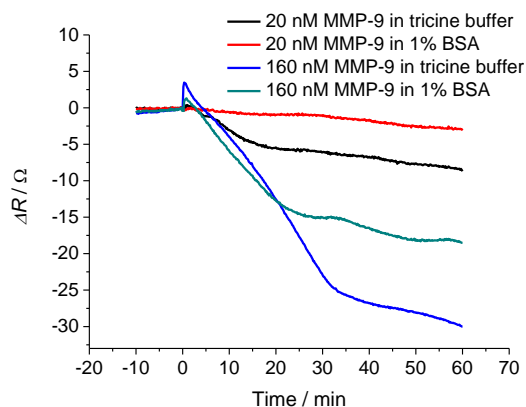
Fig. 5 QCM response, ΔR, of 25% cross-linked pOx (135 μmol/mL) to 20 nM and 160 nM MMP-9 in tricine buffer with 1% BSA.

4. Conclusions

Biosensor materials based on peptide cross-linked pOx hydrogels for disposable protease sensors were developed. The performance of the sensor material was demonstrated by using a peptide cross-linker that can be cleaved by MMP-9. The new sensor material was shown to undergo degradation after exposure to MMP-9 using QCM measurements, and the degradation was observed to be directly related to the MMP-9 concentration. Interestingly, lowering the degree of cross-linking at a lower concentration of pOx hydrogel gave a higher response towards MMP-9, which is assumed to be due to the higher porosity of the hydrogel film formed under these conditions compared to those with a higher degree of cross-linking, thereby allowing better access of the enzyme to the cleavage sites of the peptide cross-links. Using hydrogels close to the gelation point also means that a smaller number of cross-links needs to be eliminated to cause the gel to break up resulting in faster degradation. As expected from the previously reported antifouling properties of poly(2-oxazolines), the hydrogels did not show significant binding of the non-specific protein BSA, although a somewhat reduced sensitivity of the sensor in the presence of 1 % BSA was observed. This,

allied to the generic sensor format, means that the hydrogel could easily be adapted for the detection of other proteases by changing the sequence of the peptide cross-linker.

ASSOCIATED CONTENT

Supporting Information:

S1   Reaction scheme for capping method of the peptide, Ac-CSG(Ac-K)IPRRLTAC

S2   Reaction scheme for the synthesis of poly(2-oxazoline) co-polymer (pOx)

S3   Concentration of components in hydrogel formation

S4   Degradation of the modified peptide, X

S5   Demonstration of hydrogel formation

AUTHOR INFORMATION

Corresponding Author

E-mail: s.krause@qmul.ac.uk

Notes

The authors declare no competing financial interests.

Acknowledgements

References

(1)   Waubant, E.; Goodkin, D. E.; Gee, L.; Bacchetti, P.; Sloan, R.; Stewart, T.; Andersson, P.-B.; Stabler, G.; Miller, K. Serum MMP-9 and TIMP-1 Levels Are Related to MRI Activity in Relapsing Multiple Sclerosis. *Neurology* **1999**, *53* (7), 1397–1397.

(2)   Kraft-Neumärker, M.; Lorenz, K.; Koch, R.; Hoffmann, T.; Mäntylä, P.; Sorsa, T.; Netuschil, L. Full-Mouth Profile of Active MMP-8 in Periodontitis Patients. *J. Periodontal Res.* **2012**, *47* (1), 121–128.

(3)   Laugisch, O.; Schacht, M.; Guentsch, A.; Kantyka, T.; Sroka, A.; Stennicke, H. R.; Pfister, W.; Sculean, A.; Potempa, J.; Eick, S. Periodontal Pathogens Affect the Level of Protease Inhibitors in Gingival Crevicular Fluid. *Mol. Oral Microbiol.* **2012**, *27* (1), 45–56.

(4)   Xu, W.; Flores-Mireles, A. L.; Cusumano, Z. T.; Takagi, E.; Hultgren, S. J.; Caparon, M. G. Host and Bacterial Proteases Influence Biofilm Formation and Virulence in a Murine Model of Enterococcal Catheter-Associated Urinary Tract Infection. *npj Biofilms Microbiomes* **2017**, *3* (1), 28.

(5)   Guilarte, M.; Sala-Cunill, A.; Luengo, O.; Labrador-Horrillo, M.; Cardona, V. The Mast Cell, Contact, and Coagulation System Connection in Anaphylaxis. *Front. Immunol.* **2017**, *8*, 846.

(6)   Laroche, D.; Gomis, P.; Gallimidi, E.; Malinovsky, J. M.; Mertes, P. M. Diagnostic Value of Histamine and Tryptase Concentrations in Severe Anaphylaxis with Shock or Cardiac Arrest during Anesthesia. *Anesthesiology* **2014**, *121* (2), 272–279.

(7)   Riise, G. C.; Ericson, P.; Bozinovski, S.; Yoshihara, S.; Anderson, G. P.; Lindén, A. Increased Net Gelatinase but Not Serine Protease Activity in Bronchiolitis Obliterans Syndrome. *J. Hear. Lung Transplant.* **2010**, *29* (7), 800–807.

(8)   Viegas, T. X.; Bentley, M. D.; Harris, J. M.; Fang, Z.; Yoon, K.; Dizman, B.; Weimer, R.; Mero, A.; Pasut, G.; Veronese, F. M. Polyoxazoline: Chemistry, Properties, and Applications in Drug Delivery. *Bioconjug. Chem.* **2011**, *22* (5), 976–986.

(9)   Zhang, N.; Pompe, T.; Amin, I.; Luxenhofer, R.; Werner, C.; Jordan, R. Tailored Poly(2-Oxazoline) Polymer Brushes to Control Protein Adsorption and Cell Adhesion. *Macromol. Biosci.* **2012**, *12* (7), 926–936.

(10)   Konradi, R.; Acikgoz, C.; Textor, M. Polyoxazolines for Nonfouling Surface Coatings - A Direct Comparison to the Gold Standard PEG. *Macromol. Rapid Commun.* **2012**, *33* (19), 1663–1676.

(11)   Farrugia, B. L.; Kempe, K.; Schubert, U. S.; Hoogenboom, R.; Dargaville, T. R. Poly (2-Oxazoline) Hydrogels for Controlled Fibroblast Attachment. *Biomacromolecules* **2013**, *14* (8), 2724–2732.

(12)   Platen, M.; Mathieu, E.; Schubel, R.; Jordan, R.; Pautot, S. Poly (2-Oxazoline) - Based Microgel Particles for Neuronal Cell Culture. *Biomacromolecules* **2015**, *16* (5), 1516–1524.

(13)   Romio, M.; Morgese, G.; Trachsel, L.; Babity, S.; Paradisi, C.; Benetti, E. M. Poly (2-Oxazoline) -Pterostilbene Block-Copolymer Nanoparticles for Dual-Anticancer Drug Delivery. *Biomacromolecules* **2017**, *19* (1), 103–111.

(14)   Adams, N.; Schubert, U. S. Poly(2-Oxazolines) in Biological and Biomedical Application Contexts. *Advanced Drug Delivery Reviews*. 2007, pp 1504–1520.

(15)   Macgregor-Ramiasa, M.; McNicholas, K.; Ostrikov, K.; Li, J.; Michael, M.; Gleadle, J. M.; Vasilev, K. A Platform for Selective Immuno-Capture of Cancer Cells from Urine. *Biosens. Bioelectron.* **2017**, *96*, 373–380.

(16)   Anseth, K. S.; Klok, H.-A. Click Chemistry in Biomaterials, Nanomedicine, and Drug Delivery. *Biomacromolecules* **2016**, *17* (1), 1–3.

(17)   Cengiz, N., Gevrek, T. N., Sanyal, R., & Sanyal, A. Orthogonal Thiol-Ene 'Click' Reactions: A Powerful Combination for Fabrication and Functionalization of Patterned Hydrogels. *Chem. Commun.* **2017**, *53* (63), 8894–8897.

(18)   Colak, B.; Da Silva, J. C. S.; Soares, T. A.; Gautrot, J. E. Impact of the Molecular Environment on Thiol-Ene Coupling for Biofunctionalization and Conjugation. *Bioconjug. Chem.* **2016**, *27* (9), 2111–2123.

(19)   Fairbanks, B. D.; Scott, T. F.; Kloxin, C. J.; Anseth, K. S.; Bowman, C. N. Thiol−Yne Photopolymerizations: Novel Mechanism, Kinetics, and Step-Growth Formation of Highly Cross-Linked Networks. *Macromolecules* **2009**, *42* (1), 211–217.

(20)   Pereira, R. F.; Barrias, C. C.; Bártolo, P. J.; Granja, P. L. Cell-Instructive Pectin Hydrogels Crosslinked via Thiol-Norbornene Photo-Click Chemistry for Skin Tissue Engineering. *Acta Biomater.* **2018**, *66*, 282–293.

(21)   Halade, G. V.; Jin, Y. F.; Lindsey, M. L. Matrix Metalloproteinase (MMP)-9: A Proximal Biomarker for Cardiac Remodeling and a Distal Biomarker for Inflammation. *Pharmacol. Ther.* **2013**, *139* (1), 32–40.

(22)   Leifler, K. S.; Svensson, S.; Abrahamsson, A.; Bendrik, C.; Robertson, J.; Gauldie, J.; Olsson, A.-K.; Dabrosin, C. Inflammation Induced by MMP-9 Enhances Tumor Regression of Experimental Breast Cancer. *J. Immunol.* **2013**, *190* (8), 4420–4430.

(23)   Valado, A.; Leitão, M. J.; Martinho, A.; Pascoal, R.; Cerqueira, J.; Correia, I.; Batista, S.; Sousa, L.; Baldeiras, I. Multiple Sclerosis: Association of Gelatinase B/Matrix Metalloproteinase-9 with Risk and Clinical Course the Disease. *Mult. Scler. Relat.*

Disord. **2017**, *11*, 71–76.

(24) Fazio, C.; Piazzi, G.; Vitaglione, P.; Fogliano, V.; Munarini, A.; Prossomariti, A.; Milazzo, M.; D'Angelo, L.; Napolitano, M.; Chieco, P.; et al. Inflammation Increases NOTCH1 Activity via MMP9 and Is Counteracted by Eicosapentaenoic Acid-Free Fatty Acid in Colon Cancer Cells. *Sci. Rep.* **2016**, *6* (1), 20670–20679.

(25) Yabluchanskiy, A.; Ma, Y.; Iyer, R. P.; Hall, M. E.; Lindsey, M. L. Matrix Metalloproteinase-9: Many Shades of Function in Cardiovascular Disease. *Physiology (Bethesda).* **2013**, *28* (6), 391–403.

(26) Herz, J.; Zipp, F.; Siffrin, V. Neurodegeneration in Autoimmune CNS Inflammation. *Exp. Neurol.* **2010**, *225* (1), 9–17.

(27) Avolio, C.; Ruggieri, M.; Giuliani, F.; Liuzzi, G. M.; Leante, R.; Riccio, P.; Livrea, P.; Trojano, M. Serum MMP-2 and MMP-9 Are Elevated in Different Multiple Sclerosis Subtypes. *J. Neuroimmunol.* **2003**, *136* (1–2), 46–53.

(28) Benešová, Y.; Văkǒ, A.; Novotná, H.; Litzman, J.; Štourač, P.; Beránek, M.; Kadaňka, Z.; Bednařák, J. Matrix Metalloproteinase-9 and Matrix Metalloproteinase-2 as Biomarkers of Various Courses in Multiple Sclerosis. *Mult. Scler.* **2009**, *15* (3), 316–322.

(29) Trentini, A.; Castellazzi, M.; Cervellati, C.; Manfrinato, M. C.; Tamborino, C.; Hanau, S.; Volta, C. A.; Baldi, E.; Kostic, V.; Drulovic, J.; et al. Interplay between Matrix Metalloproteinase-9, Matrix Metalloproteinase-2, and Interleukins in Multiple Sclerosis Patients. *Dis. Markers* **2016**, *2016*, 1–9.

(30) Stair, J. L.; Watkinson, M.; Krause, S. Sensor Materials for the Detection of Proteases. *Biosens. Bioelectron.* **2009**, *24* (7), 2113–2118.

(31)   Sumner, C.; Krause, S.; Sabot, A.; Turner, K.; McNeil, C. J. Biosensor Based on Enzyme-Catalysed Degradation of Thin Polymer Films. *Biosens. Bioelectron.* **2001**, *16* (9–12), 709–714.

(32)   Zheng, X.; Cook, J. P.; Watkinson, M.; Yang, S.; Douglas, I.; Rawlinson, A.; Krause, S. Generic Protease Detection Technology for Monitoring Periodontal Disease. *Faraday Discuss.* **2011**, *149*, 37–47.

(33)   Kamarun, D.; Zheng, X.; Milanesi, L.; Hunter, C. A.; Krause, S. A Peptide Cross-Linked Polyacrylamide Hydrogel for the Detection of Human Neutrophil Elastase. *Electrochim. Acta* **2009**, *54* (22), 4985–4990.

(34)   Millington, R. B.; Mayes, A. G.; Blyth, J.; Lowe, C. R. A Holographic Sensor for Proteases. *Anal. Chem.* **1995**, *67* (23), 4229–4233.

(35)   Saum, A. G. .; Cumming, R. .; Rowell, F. . Use of Substrate Coated Electrodes and AC Impedance Spectroscopy for the Detection of Enzyme Activity. *Biosens. Bioelectron.* **1998**, *13* (5), 511–518.

(36)   Hanumegowda, N. M.; White, I. M.; Oveys, H.; Fan, X. Label-Free Protease Sensors Based on Optical Microsphere Resonators. *Sens. Lett.* **2005**, *3* (4), 315–319.

(37)   Krause, S.; Mcneil, C. J.; Fernández-sánchez, C.; Sabot, A. Sensors Based on Thin Film Degradation. In *Encyclopedia of Sensors*; American Scientific Publishers, 2006; pp 289–306.

(38)   Schyrr, B.; Boder-Pasche, S.; Ischer, R.; Smajda, R.; Voirin, G. Fiber-Optic Protease Sensor Based on the Degradation of Thin Gelatin Films. *Sens. Bio-Sensing Res.* **2015**, *3*, 65–73.

(39)   Biela, A.; Watkinson, M.; Meier, U. C.; Baker, D.; Giovannoni, G.; Becer, C. R.;

Krause, S. Disposable MMP-9 Sensor Based on the Degradation of Peptide Cross-Linked Hydrogel Films Using Electrochemical Impedance Spectroscopy. *Biosens. Bioelectron.* **2015**, *68*, 660–667.

(40) Ahmad, N.; Colak, B.; Zhang, D.-W.; Gibbs, M. J.; Watkinson, M.; Becer, C. R.; Gautrot, J. E.; Krause, S. Peptide Cross-Linked Poly (Ethylene Glycol) Hydrogel Films as Biosensor Coatings for the Detection of Collagenase. *Sensors* **2019**, *19* (7), 1677 (1-9).

(41) Pei, P.; Horan, M. P.; Hille, R.; Hemann, C. F.; Schwendeman, S. P.; Mallery, S. R. Reduced Nonprotein Thiols Inhibit Activation and Function of MMP-9: Implications for Chemoprevention. *Free Radic. Biol. Med.* **2006**, *41* (8), 1315–1324.

(42) Khrenova, M. G.; Savitsky, A. P.; Topol, I. A.; Nemukhin, A. V. Exploration of the Zinc Finger Motif in Controlling Activity of Matrix Metalloproteinases. *J. Phys. Chem. B* **2014**, *118* (47), 13505–13512.

(43) Gress, A.; Völkel, A.; Schlaad, H. Thio-Click Modification of Poly[2-(3-Butenyl)-2-Oxazoline]. *Macromolecules* **2007**, *40* (22), 7928–7933.

(44) Schenk, V.; Ellmaier, L.; Rossegger, E.; Edler, M.; Griesser, T.; Weidinger, G.; Wiesbrock, F. Water-Developable Poly(2-Oxazoline)-Based Negative Photoresists. *Macromol. Rapid Commun.* **2012**, *33* (5), 396–400.

(45) Megone, W.; Roohpour, N.; Gautrot, J. E. Impact of Surface Adhesion and Sample Heterogeneity on the Multiscale Mechanical Characterisation of Soft Biomaterials. *Sci. Rep.* **2018**, *8* (1), 6780.

(46) Sabot, A.; Krause, S. Simultaneous Quartz Crystal Microbalance Impedance and Electrochemical Impedance Measurements. Investigation into the Degradation of Thin

Polymer Films. *Anal. Chem.* **2002**, *74* (14), 3304–3311.

(47) Kridel, S. J.; Chen, E.; Kotra, L. P.; Howard, E. W.; Mobashery, S.; Smith, J. W. Substrate Hydrolysis by Matrix Metalloproteinase-9. *J. Biol. Chem.* **2001**, *276* (23), 20572–20578.

(48) Chen, E. I.; Li, W.; Godzik, A.; Howard, E. W.; Smith, J. W. A Residue in the S2 Subsite Controls Substrate Selectivity of Matrix Metalloproteinase-2 and Matrix Metalloproteinase-9. *J. Biol. Chem.* **2003**, *278* (19), 17158–17163.

(49) Adibnia, V.; Hill, R. J. Universal Aspects of Hydrogel Gelation Kinetics, Percolation and Viscoelasticity from PA-Hydrogel Rheology. *J. Rheol. (N. Y. N. Y).* **2016**, *60* (4), 541–548.

(50) Castner, D. G.; Hinds, K.; Grainger, D. W. X-Ray Photoelectron Spectroscopy Sulfur 2p Study of Organic Thiol and Disulfide Binding Interactions with Gold Surfaces. *Langmuir* **1996**, *12* (21), 5083–5086.

(51) Bourg, M.-C.; Badia, A.; Lennox, R. B. Gold−Sulfur Bonding in 2D and 3D Self-Assembled Monolayers: XPS Characterization. *J. Phys. Chem. B* **2000**, *104* (28), 6562–6567.

(52) Zhang, L.; Ji, L.; Glans, P.-A.; Zhang, Y.; Zhu, J.; Guo, J. Electronic Structure and Chemical Bonding of a Graphene Oxide–sulfur Nanocomposite for Use in Superior Performance Lithium–sulfur Cells. *Phys. Chem. Chem. Phys.* **2012**, *14* (39), 13670–13675.

(53) Gobbo, P.; Biesinger, M. C.; Workentin, M. S. Facile Synthesis of Gold Nanoparticle (AuNP)–carbon Nanotube (CNT) Hybrids through an Interfacial Michael Addition Reaction. *Chem. Commun.* **2013**, *49* (27), 2831–2833.

TOC

Protease detection through degradation of peptide cross-links